Sensors and Actuators A 171 (2011) 146–151

Contents lists available at ScienceDirect

Sensors and Actuators A: Physical

journal homepage: www.elsevier.com/locate/sna

The properties of lattice-shifted microcavity in photonic crystal slab and its applications for electro-optical sensor

Daquan Yang[a,b], Huiping Tian[a,b], Yuefeng Ji[a,b,*]

[a] The State Key Laboratory of Information Photonics and Optical Communications, Beijing 100876, China
[b] School of Information and Communication Engineering, Beijing University of Posts and Telecommunications, Beijing, China

ARTICLE INFO

Article history:
Received 28 February 2011
Received in revised form 1 August 2011
Accepted 1 August 2011
Available online 4 August 2011

Keywords:
Photonic crystals
Electro-optical sensor
Lattice-shifted microcavity
Waveguide
SOI

ABSTRACT

In this paper, a micro electro-optic sensor structure and its sensing technique based on lattice-shifted resonant microcavity (H0-nanocavity) in a triangular lattice photonic crystals (PhCs) slab are presented. The H0-nanocavity is formed by only laterally shifting two adjacent holes outwards slightly in the opposite direction, which can realize a nanocavity with high quality factor (Q) value to meet the requirements of practical application. The electro-optic sensor is realized in hole-array based photonic crystal slab with triangular lattice air holes infiltrated with a nonlinear optical (NLO) polymer (n_{poly} = 1.6) in Silicon-on-Insulator (SOI) operating in the wavelength range from 1400 nm to 1600 nm. The simulation results of PhC electro-sensitive structure show that the optical properties of PhCs can be used to design sensing devices characterized by a high degree of compactness and good resolution. The properties of the sensor are analyzed and calculated using the plane-wave expansion (PWE) method and simulated using the finite-difference time-domain (FDTD) method. The simulation results display that the resonant wavelength of the mode localized in the microcavity shifts its spectral drop position following a linear behavior when a driving voltage ranging between 0.0 V and 3.2 V is applied, and the sensitivity of 31.90 nm/V is observed.

1. Introduction

Over the past decade, photonic crystal (PhC) is considered as a kind of periodic dielectric structure with the capability to manipulate light propagation, for instance Refs. [1,2]. Photonic crystal has been studied extensively for many applications such as electro-optical modulation [3–6], high-resolution sensors [7–9], ultra-small filters [10–12], low-threshold nanolasers [13], quantum information processing [14], and group delay [15]. Their application as sensors is a recent research field which seems to be very promising due to their extreme miniaturization, high spectral sensitivity and MEMS (Micro-Electro-Mechanical System) integration. Thus there has been a dramatic increase in the level of interest regarding the ultra-compact and high-sensitivity micro sensors. So far, with the further research, large number of architectures regarding to micro sensor based on PhC technology have been proposed in works and researches on various sensors with different functions, such as stress sensor [16,17], micro displacement sensor [18–21] and biochemical sensor [22–29]. In addition, the development of nanotechnologies makes it possible to fabricate photonic crystal structures on the scale of tens to hundreds of nanometers, which have been previously shown to work from solution [30,31].

In practice, a 2-dimensional (2D) photonic crystal slab has emerged as one of the most important platforms to fabricate a high quality factor (Q) optical microcavity, such as Ln cavity [32], mode-gap cavity [33], and H0 nanocavity [34] used in this paper. Recently, most of the reported 2D PhC based microcavities are formed from periodic air hole-array. Because of that relative to the pillar-array based PhC [35], hole-array based PhC usually selectively removed the material underneath the cavity to form a similar free-standing membrane which can better reduce the vertical leakage into the substrate than the pillar-array based PhC cavity could do. Additionally, a pillar array based 2D PhC is difficult to form a similar free-standing membrane. At the same time, it is well-known that a triangular lattice PhC can create the PBG more easily than the square lattice PhC. Hence, the basic structural unit of electro-optic sensor designed in this paper is based on triangular lattice, hole-array based PhC. In addition, two micro electrodes are placed on each side of the PhC waveguide.

In this paper we report the design and simulations of a PhC electro-sensitive device consisting of a PhC waveguide (PhCW, here is W1 waveguide) coupled to a PhC microcavity obtained by shifting two lattice points in a triangular lattice PhC slab to create a point defect in the regular 2D periodic pattern. The waveguide is designed

* Corresponding author at: Beijing University of Posts and Telecommunications, P.O. Box 90, #10 Xitucheng Road, Haidian District, Beijing 100876, China.
E-mail addresses: yangdq5896@163.com (D. Yang), hptian@bupt.edu.cn (H. Tian), jyf@bupt.edu.cn (Y. Ji).

0924-4247/$ – see front matter © 2011 Elsevier B.V. All rights reserved.
doi:10.1016/j.sna.2011.08.001

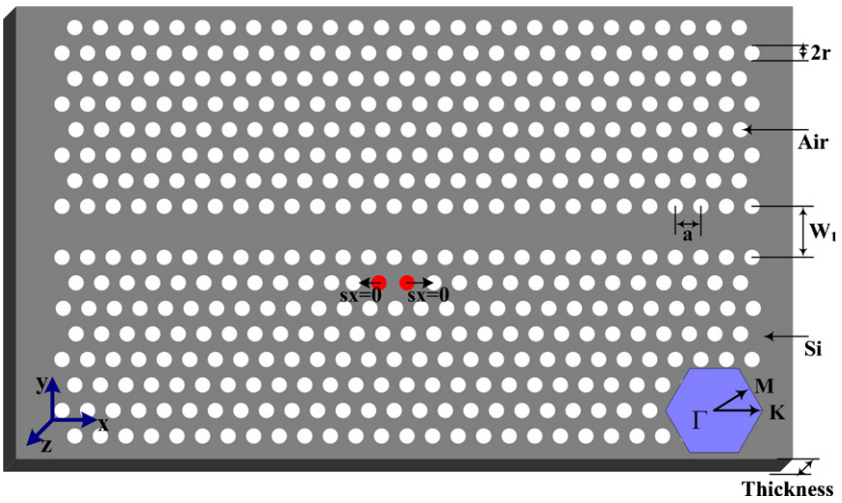

Fig. 1. Structure model of W1 PhC slab waveguide without a microcavity, where $a = 403$ nm, $r = 0.32a$, $T = 0.55a$. The red holes are the shifted holes forming a resonant cavity, and here the lattice shift $sx = 0$. (For interpretation of the references to colour in this figure legend, the reader is referred to the web version of the article.)

in order to allow the propagation to obtain a large effective wavelength range in photonic band gap (PBG). The coupling with the point defect causes a sharp drop in the transmittance spectrum corresponding to the microcavity resonance wavelength. When an extra driving voltage is applied to the PhC sensor sample, a variation in the refractive index of the nonlinear optical (NLO) polymer infiltrated in the air holes of the PhC slab occurs due to the electro-optical effect in electro-optic crystals. This simultaneously modifies the optical properties of the cavity, thus shifting the resonant wavelength in the transmittance spectrum. The amount of such spectral displacement can be therefore exploited to measure the applied driving voltage. Particularly, the numerical results, obtained by the 3D-FDTD method, illustrate that the spectral position of the resonating drop detected at the output of the PhCW shifts towards lower wavelengths as the driving voltage value increases. The shift linearly depends on the applied driving voltage, being displaced of about 31.90 nm/V.

The whole organization of this paper is as follows. In Section 2, we first introduced the PhC slab lattice-shifted microcavity (H0-nanocavity) structural model and some corresponding simulation data. Then, in Section 3 we analyzed the electro-optical effect and the simulation method of the electro-optical sensor based on W1 waveguide coupled to a PhC microcavity structure, and at the same time, the sensitivity of the PhC sensor was discussed and obtained with the different applied driving voltages. Finally, in Section 4, we drew a brief conclusion.

2. The basic structural unit design of electro-optical sensor

In this section, we will introduce how to design the basic structural unit of an electro-optic sensor which consists of a microcavity coupled to a PhC single line defect waveguide (W1). Firstly, in Section 2.1 we introduce the design of the W1 PhC slab waveguide which can realize a large enough photonic band gap and confine the TE-like polarized light strongly in both in-plane direction and out-plane direction. Then we introduce how to design the resonant microcavity (H0-nanocavity) which can better couple to W1 PhC slab waveguide in Section 2.2.

2.1. Design of the W1 PhC slab waveguide without microcavity (sx = 0)

The basic structural unit of electro-optic sensor designed in our paper is based on triangular lattice, hole-array based PhC, and shown as Fig. 1. It is constructed in a silicon slab ($n_{si} = 3.48$) by arranging a triangular lattice of air holes, where the central row of air holes are removed in order to form a line defect (W1) waveguide. The red holes are used as shifting holes to form a resonant cavity coupled to the W1 waveguide, and here the lattice shift $sx = 0$ (Fig. 1).

In Fig. 1 we can see that the W1 PhC slab waveguide without microcavity ($sx = 0$) is modeled by a PhC single line defect waveguide (W1) with a triangular lattice of air holes, having lattice constant $a = 403$ nm, radius of air holes $r = 0.32a = 128.96$ nm and slab thickness $T = 0.55a = 221.65$ nm realized on silicon slab.

In this paper, regarding to the 2D PhC slab (considering the thickness), the properties of the sensor are analyzed and calculated using the plane-wave expansion (PWE) method and simulated using the finite-difference time-domain (FDTD) method to calculate the 2D PhC slab's photonic band and transmittance spectrum, respectively. The analysis performed in this work has concentrated on the TE-like polarization, for which the PhC structure exhibits a large band gap (PBG) [36]. A typical band diagram for TE-like polarized light in the single line defect waveguide PhC is obtained numerically by using the plane wave expansion method when the lattice shift $sx = 0$, and shown in Fig. 2.

As seen in Fig. 2, the PhC waveguide supports one even mode and odd mode in the photonic band gap which ranges about from $0.206(2\pi c/a)$ to $0.285(2\pi c/a)$. Since the even mode is seen to flatten

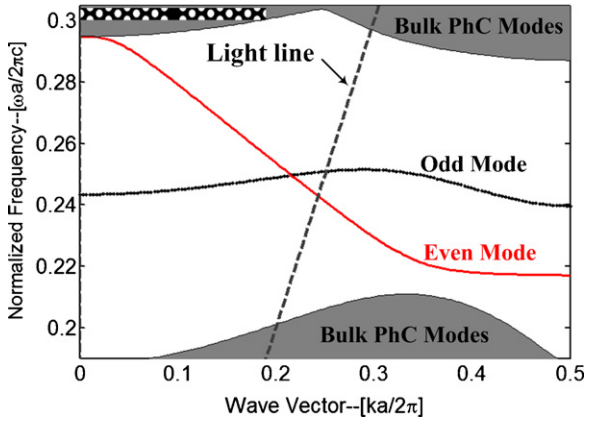

Fig. 2. Photonic band of a W1 PhC with the shift $sx = 0$ for the TE-like polarization; insert is the unit cell.

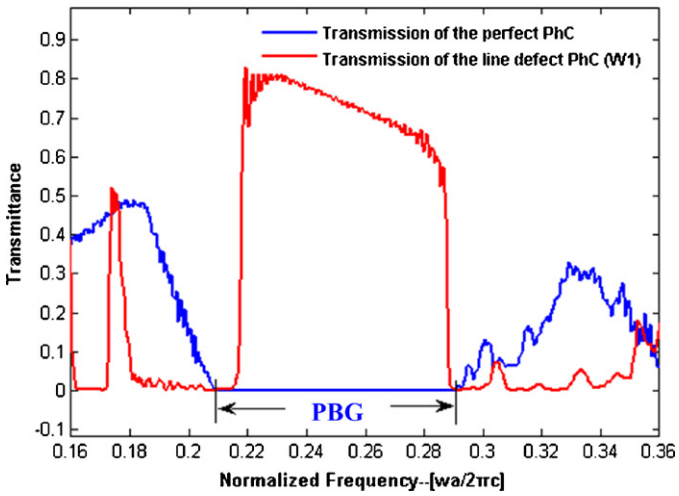

Fig. 3. The transmission spectrum of TE-like polarized light wave in the line defect PhC and perfect PhC. The red line is the transmission in the line defect PhC when the shift $sx = 0$; the blue line is the transmission in the perfect PhC without any defect. (For interpretation of the references to colour in this figure legend, the reader is referred to the web version of the article.)

at large wave vectors due to the folding at the Brillouin zone-end, in our numerical calculation, the simulated transmission is calculated based on the even mode. We can also see that when the normalized frequency exceeds $0.24(2\pi c/a)$, the even mode is lying above the light line (in the radiation mode region) and leakage in the vertical direction will increase (compared to the even mode lying below the light line). That is in complete accordance with the results shown in Fig. 3. As shown in Fig. 3 when the normalized frequency exceeds $0.24(2\pi c/a)$, the transmission decreases. However, as proven in previous work, with careful design about the structure parameters such as lattice constant, radius of the holes, and thickness of the slab as shown in Fig. 1, the loss in the vertical direction could be reduced. And the relevant simulation results of the light propagation through the PhC slab waveguide with lattice shift $sx = 0$ in Fig. 1 are shown in Fig. 4. As seen in Fig. 4, the TE-like polarized light is confined strongly in both in-plane direction and out-plane direction, and the leakage of light is very small.

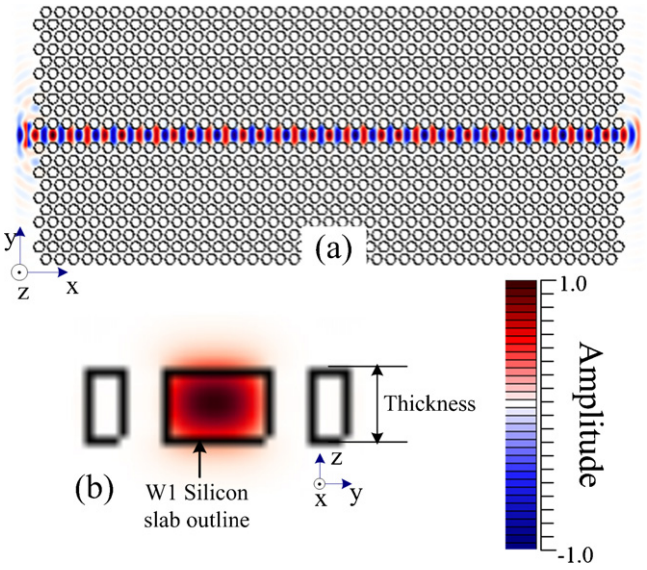

Fig. 4. Steady state electric field profile for the fundamental TE-like mode propagating through a PhC waveguide with shifting $sx = 0$ in the (a) x–y plane; (b) y–z plane.

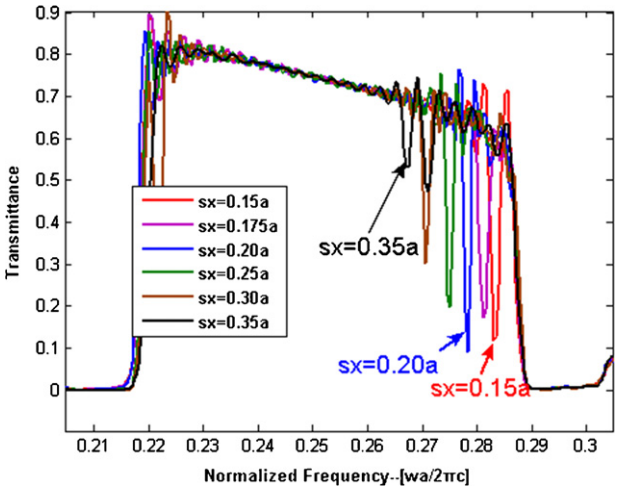

Fig. 5. Output transmission spectrum of TE-like polarized light wave in the basic structural unit of electro-optic sensor with the different lattice shifts ranging from $sx = 0.15a$ to $0.35a$.

2.2. Design of the microcavity coupled to W1 PhC slab waveguide

In this paper, based on the W1 PhC slab waveguide structure, we increase the Q-factor of the device by using the high-Q microcavity (lattice-shifted microcavity) which is designed by only shifting the two red holes outwards slightly in the opposite direction around the W1 waveguide as shown in Fig. 1. In Ref. [16], the microcavity demonstrated by Stomeo et al. is used in the fabrication of force sensors based on 2D photonic crystal, where the microcavity was formed by changing parameters of more than six holes around the W1 waveguide. However, the microcavity used in this design is formed by only shifting the two red holes outwards slightly in the opposite direction around the W1 waveguide (Fig. 1). In view of the higher accuracy and simpler implementation, the design of the microcavity presented in this paper seems to be more appropriate for practical design. In addition, it can also create a sharp drop in transmission spectrum and achieve Q-factors as high as in the order of 10^5 given in [37] to meet the requirements of practical application. At the same time, it provides a better coupling between the W1 waveguide and the resonant cavity and improves the Q factor of the microcavity because of the envelope function of the in-plane mode profile varies more gently than the single defect case.

With the different lattice shifts of sx, the resonant frequency between the resonant cavity and the W1 PhC waveguide will shift. As sx increases from $sx = 0.15a$ to $0.35a$, the simulation results reveal that the position of resonating drop detected at the output of the PhC waveguide shifts towards lower frequency. The detailed simulation result is shown in Fig. 5. As seen in Fig. 5, when the shift $sx = 0.2a$, the coupling strength between the microcavity and the W1 PhC waveguide is maximum in the PhC slab microcavity structure.

3. Electro-optic effect analysis and simulation results

In our proposed electro-optical (EO) sensor based on the PhC slab, which consists of a line defect PhC waveguide (W1) coupled to a resonant cavity obtained by creating a point defect in the regular 2D periodic pattern as shown in Fig. 6. Here, the air holes are infiltrated with a nonlinear optical (NLO) polymer ($n_{poly} = 1.6$) [5,6], which can be purchased commercially. First of all, EO effect via NLO polymers allows extremely high response speeds extending up to frequencies in the terahertz range [38]. Furthermore, molecular engineering of organic EO materials has led to extremely high Pockels coefficients in polymers, exceeding 300 pm/V [39],

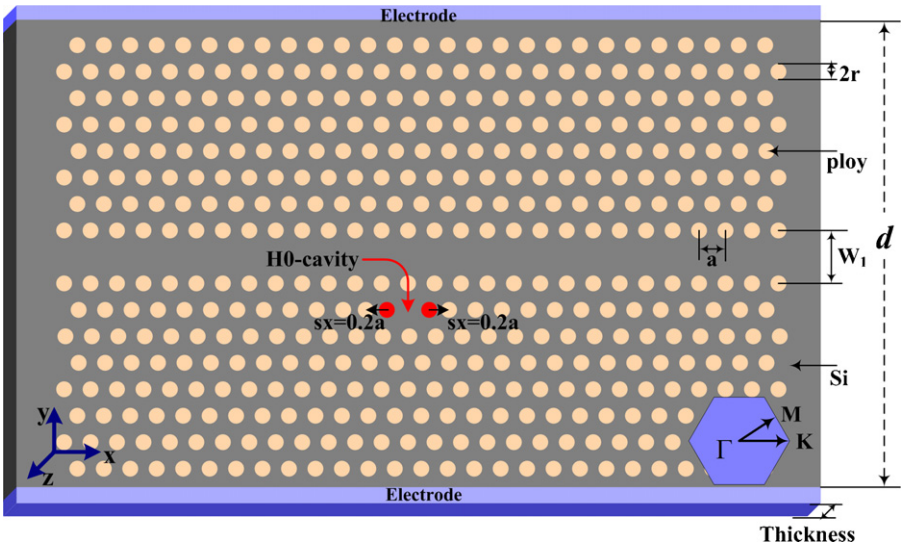

Fig. 6. Structural model of electro-optic sensor based on W1 PhC slab microcavity coupled to the photonic crystal, where $a = 403$ nm, $r = 0.32a$, $T = 0.55a$, $sx = 0.2a$. The red holes and the bulk holes (orange holes) are all infiltrated with NLO polymer ($n_{poly} = 1.6$). (For interpretation of the references to colour in this figure legend, the reader is referred to the web version of the article.)

which is 10 times the value available in lithium niobate as the standard in organic material used in EO applications. Photonic devices based on a hybrid material system merging silicon and polymer are therefore attractive, since they combine the strong light-confining abilities of silicon with the superior NLO properties of polymers. In addition, concepts based on PhC waveguides can exploit high quality factor (Q) cavities or slow-light mechanisms to achieve very compact device dimensions and have been discussed [40,41]. So, through the design of the basic structural unit of electro-optic sensor discussed in Section 2, the electro-sensitive sensor reported in this paper consists of a PhC single line defect waveguide (W1) coupled to a resonant cavity obtained by creating a point defect in the regular 2D periodic pattern. Here, the triangular lattice PhC is realized on silicon slab ($n_{si} = 3.48$) in Silicon-on-Insulator (SOI) with air holes infiltrated with a nonlinear optical (NLO) polymer ($n_{poly} = 1.6$) which is required to be poled before becoming electro-optically active [5,6,41], and having lattice constant $a = 403$ nm, radius $r = 0.32a = 128.96$ nm and the slab thickness $T = 0.55a = 221.65$ nm. In addition, two micro electrodes are placed on each side of the PhC waveguide, which means that the electrostatic field lines are parallel to the y axis, allowing the largest electro-optic coefficient in polystyrene to be used. The lattice-shifted microcavity (H0-nanocavity) is designed by only laterally shifting the two red holes slightly ($sx = 0.2a$) in the opposite direction along the PhC waveguide as shown in Fig. 6.

Based on the electro-optic sensor's architecture shown in Fig. 6, by applying the 3D-FDTD method, with the structure excited by an input Gaussian pulse characterized by a wide spectrum centered at $\omega = 0.25(2\pi c/a)$, the simulation of light propagation through the electro-sensitive structure in the x–y plane and the output transmission spectrum of TE-like polarized light wave in W1 PhC waveguide is numerically calculated, as plotted in Figs. 7 and 8.

Now we are in a position to investigate the modification of band gap in a photonic bandgap structure undergoing driving voltage (U) application. The operation principle of the PhC slab electro-optic sensor is based on the fact that the driving voltage application provokes a change in the refractive index of the polymer which modifies the output transmission spectrum of the regular photonic crystal or that of the localized state when a defected photonic crystal is considered.

Fundamentally, the electric-optical sensor system is based on the linear electro-optic effect (Pockel's effect) in electro-optic crystals where a pulsed microwave signal acts as a transient bias to induce a transient polarization in the sensor crystal. This polarization causes a change in the index of refraction. The change in refractive index is then probed by a synchronously pulsed laser beam, and then converted into an amplitude modulation. In the small signal regime, amplitude variation of the optical probe beam is proportional to the applied electric field. If the driving voltage varies, the refractive index of polymer will be changed because of the Pockel's effect. To model the driving voltage action, the change

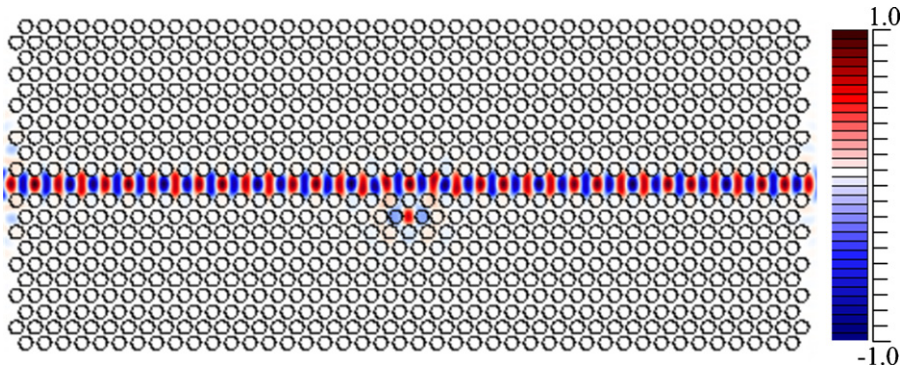

Fig. 7. Steady state electric field profile for the fundamental TE-like mode propagating through the electro-sensitive structure in the x–y plane.

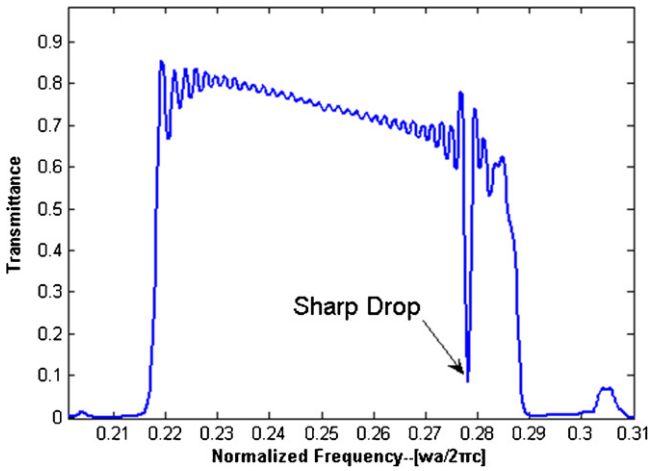

Fig. 8. Output transmission spectrum of TE-like polarized light wave in the electro-sensitive structure in absence of applied driving voltage.

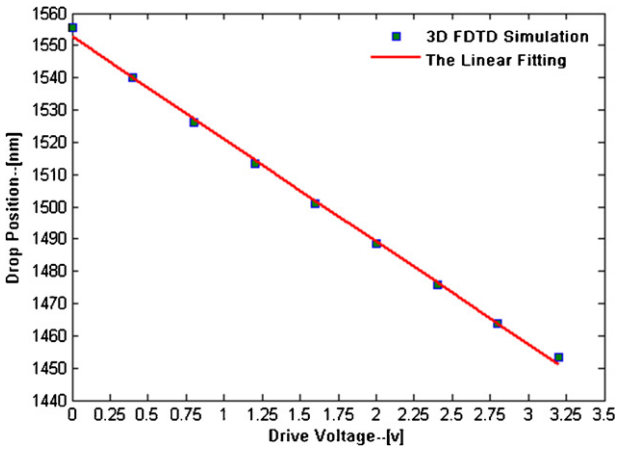

Fig. 10. The shift of output drop resonance wavelength as a function of the applied drive voltage of PhC electro-optic sensor structure.

in the refractive index (Δn) of the polymer due to the electro-optic effects acting on the NLO polymer infiltrated in the PhC holes has been evaluated. The final expression for the relationship between the variation in the refractive index of polymer (Δn) and the driving voltage (U) is expressed as follow [6]:

$$\Delta n = -\frac{1}{2} \times n_{poly}^3 \times \gamma_{33} \times \frac{U}{d} \quad (1)$$

where γ_{33} is the electro-optic coefficient, U is the applied driving voltage and d represents the spacing between the electrodes. We choose a state-of-the-art polymer material with γ_{33} = 150 pm/V [5].

Based on the electro-optic sensor's architecture as shown in Fig. 6, simulation results show that the refractive index change of the polymer is mainly due to the electro-optic effects when a driving voltage is applied normally to the plane of PhC slab. By applying the 3D-FDTD method, we calculate the output transmission spectrum for different values of the applied driving voltage. The drop peak corresponds to the resonant wavelength of the mode localized in the PhC slab microcavity, and it shifts its spectral position, following a linear relation when a driving voltage ranging between 0.0 V and 3.2 V with step ΔU = 0.4 V is applied. The output transmission spectrum for different driving voltages ranging from 0 V to 3.2 V is shown in Fig. 9. As seen in Fig. 9, it reveals that the spectral position of the resonating drop detected at the output of the PhC

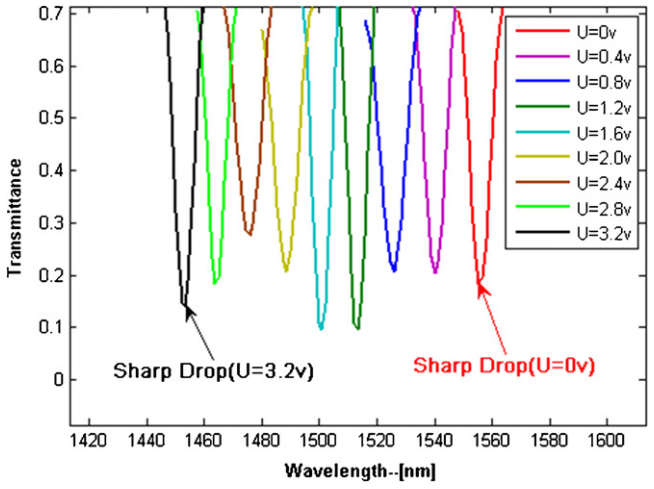

Fig. 9. The sharp drop fraction of output transmission spectrum for different applied driving voltages ranging between 0 V and 3.2 V.

waveguide shifts towards lower wavelengths as the applied voltage value is increased.

Here to analyze the sensitivity (S) of the PhC electro-optic sensor, we define the sensitivity of our electro-optic sensor device by observing the shift in the resonant wavelength ($\Delta\lambda$) as a function of the change in applied driving voltage (ΔU) of the PhC electro-optic sensor structure as shown in Fig. 10. The electro-optic sensor's sensitivity is expressed as:

$$S = \frac{\Delta\lambda}{\Delta U} \quad (2)$$

As seen in Fig. 10, there is a linear relationship between the output drop resonant wavelength and the applied driving voltage. From the simulation data shown in Figs. 9 and 10, it is possible to calculate the sensor sensitivity that is equal to 31.90 nm/V. In addition, based on Eq. (1) we also can calculate that a refractive index change of just Δn = 0.001 results in a wavelength red shift of approximately $\Delta\lambda$ = 0.18 nm (refractive index (RI) sensitivity is ~180 nm/RIU). Compared to the slotted photonic crystal waveguide based Electro-Optical Modulator demonstrated by Wülbern et al. [5], where the $\Delta\lambda$ is 0.12 nm as refractive index change of Δn = 0.001, the device presented in this paper is improved. At the same time, compared to photonic crystals slab sensor with multiple-hole defects (MHDs) photonic crystal cavities demonstrated by Kang et al. [42], the sensor with lattice-shifted cavity in this paper enabled an 80% increase in detection sensitivity towards bulk refractive index. This strong sensitivity is a result of the electric field enhancement in the H0-nanocavity region with the small mode volume (Fig. 7).

4. Conclusions

In summary, we have proposed to apply the electro-optic properties of photonic crystals to realize electro-optic sensing devices characterized by an ultra-compact and a good resolution. We confirmed the characteristics of electro-optic sensor by designing and simulating a silicon waveguide PhC slab microcavity for the wavelength range 1400–1600 nm, with the sensitivity is equal to 31.90 nm/V. This sensitivity could be further improved by either maximizing the quality factor of the resonance state or by fabricating the same 2D PhC structure on a membrane configuration. It is worth mentioning that the microcavity used in our design is formed by only laterally moving the two adjacent holes around the W1 waveguide outwards slightly in the opposite direction, which is relatively simple and will be easier and more accurately designed in

practical applications compared to the microcavity demonstrated by Stomeo et al. used in the fabrication of force sensor [16].

In addition, it is noteworthy that the same micro-sensor architecture can be integrated on the single silicon substrate to constitute a micro-sensor array, which enables the realization of sensors covering a broad sensing range and versatile functions. This subject is under investigation.

Acknowledgements

This research was supported in part by National 973 Program (No. 2011CB302702, No.2012CB315705), National 863 Program (No. 2009AA01A345), and NSFC (No. 60932004), P. R. China.

References

[1] T. BaBa, Slow light in photonic crystals, Nat. Photonics 2 (2008) 465–473.
[2] A. Vlasov, M. Boyle, H. Hamann, J. McNab, Active control of slow light on a chip with photonic crystal waveguides, Nature 438 (2005) 65–69.
[3] C.-Y. Lin, X.L. Wang, S. Chakravarty, B.S. Lee, W. Lai, J. Luo, A.K.-Y. Jen, R.T. Chen, Electro-optic polymer infiltrated silicon photonic crystal slot waveguide modulator with 23 dB slow light enhancement, Appl. Phys. Lett. 97 (2010) 093304.
[4] X. Chen, A. Lan, X. Wang, T. Chen, Electro-optically active slow light enhanced silicon slot photonic crystal waveguides, IEEE J. Sel. Top. Quant. Electron 15 (2009) 1506–1509.
[5] J.H. Wülbern, A. Petrov, M. Eich, Electro-optical modulator in a polymer-infiltrated silicon slotted photonic crystal waveguide heterostructure resonator, Opt. Express 17 (2009) 304–313.
[6] J.M. Brosi, C. Koos, L.C. Andreani, M. Waldow, J. Leuthold, W. Freude, High-speed low-voltage electro-optic modulator with a polymer-infiltrated silicon photonic crystal waveguide, Opt. Express 16 (2008) 4177–4191.
[7] A. Di Falco, L. O'Faolain, T.F. Krauss, Slotted photonic crystal waveguides and cavities for slow light and sensing applications, in: IEEE International Conference, vol. 5, 2008.
[8] M.A. Dündar, C.I. Ryckebosch, R.N. Fouad Karouta, L.J. Jzendoorn, W. Rob, Sensitivities of InGaAsP photonic crystal membrane nanocavities to hole refractive index, Opt. Express 18 (2010) 4049–4056.
[9] X.L. Wang, Zh.F. Xu, N.G. Lu, J. Zhu, F. Jin, Ultracompact refractive index sensor based on microcavity in the sandwiched photonic crystal waveguide structure, Opt. Commun. 281 (2008) 1725–1731.
[10] S. Noda, A. Chutinan, M. Imada, Trapping and emission of photons by a single defect in a photonic bandgap structure, Nature 407 (2000) 608–610.
[11] B.S. Song, S. Noda, T. Asano, Photonic devices based on in-plane hetero photonic crystals, Science 300 (2003) 1537.
[12] H. Takano, Y. Akahane, T. Asano, S. Noda, In-plane-type channel drop filter in a two-dimensional photonic crystal slab, Appl. Phys. Lett. 84 (222) (2004) 6–2228.
[13] O. Painter, R.K. Lee, A. Scherer, A. Yariv, J.D. O'Brien, P.D. Dapkus, I. Kim, Two-dimensional photonic band-gap defect mode laser, Science 284 (1999) 1819–1821.
[14] P. Michler, A. Kiraz, C. Becher, W.V. Schoenfeld, P.M. Petroff, L. Zhang, E. Hu, A. Imamoğlu, A quantum dot single-photon turnstile device, Science 290 (2000) 2282–2285.
[15] M.F. Yanik, S. Fan, Stopping light all optically, Phys Rev. Lett. 92 (2004) 083901–083904.
[16] T. Stomeo, M. Grande, A. Qualtieri, A. Passaseo, A. Salhi, M. DeVittorio, D. Biallo, A. Dorazio, M. DeSari, V. Marrocco, V. Petruzzelli, F. Prudenzano, Fabrication of force sensors based on two-dimensional photonic crystal technology, Microelectron. Eng. 84 (2007) 1450–1453.
[17] T. Lu, P.T. Lee, Ultra-high sensitivity optical stress sensor based on double layered photonic crystal microcavity, Opt. Express 17 (2009) 1518–1526.
[18] Zh.F. Xu, L.C. Cao, C. Gu, Q.H. He, G.F. Jin, Micro displacement sensor based on line-defect resonant cavity in photonic crystal, Opt. Express 14 (2006) 298–305.
[19] O. Levy, B.Z. Steinberg, M. Nathan, A. Boag, Ultrasensitive displacement sensing using photonic crystal waveguides, Appl. Phys. Lett. 86 (10410) (2005) 2–104104.
[20] W. Suh, M.F. Yanik, O. Solgaard, S. Fan, Displacement-sensitive photonic crystal structures based on guided resonance in photonic crystal slabs, Appl. Phys. Lett. 82 (199) (2003) 9–2001.
[21] W. Suh, O. Solgaard, S. Fan, Displacement sensing using evanescent tunneling between guided resonances in photonic crystal slabs, J. Appl. Phys. 98 (03310) (2005) 2–033105.
[22] S.C. Buswell, V.A. Wright, J.M. Buriak, V. Van, S. Evoy, Specific detection of proteins using photonic crystal waveguides, Opt. Express 16 (2008) 15949–15957.
[23] C.A. Barrios, M.J. Bañuls, V. González-Pedro, K.B. Gylfason, B. Sánchez, A. Griol, A. Maquieira, H. Sohlström, M. Holgado, R. Casquel, Label-free optical biosensing with slot-waveguides, Opt. Lett. 33 (2008) 708–710.
[24] M. Lee, P.M. Fauchet, Two dimensional silicon photonic crystal based biosensing platform for protein detection, Opt. Express 15 (2007) 4530–4535.
[25] A. DiFalco, L. OFaolain, T.F. Krauss, Chemical sensing in slotted photonic crystal heterostructure cavities, Appl Phys. Lett. 94 (2009) 063503–063505.
[26] A.M. Armani, R.P. Kulkarni, S.E. Fraser, R.C. Flagan, K.J. Vahala, Label-free single-molecule detection with optical microcavities, Science 317 (2007) 783–787.
[27] S. Pal, E. Guillermain, R. Sriram, B.L. Miller, P.M. Fauchet, Silicon photonic crystal nanocavity-coupled waveguides for error-corrected optical biosensing, Biosens. Bioelectron. 26 (2011) 4024–4031.
[28] F. Hsiao, C. Lee, Nanophotonic biosensors using hexagonal nano-ring resonators—a computational study, SPIE J. Micro/Nanolithogr. 10 (2011) 013001, MEMS MOEMS (JM3).
[29] F. Hsiao, C. Lee, Computational study of photonic crystals nano-ring resonator for biochemical sensing, IEEE Sens. J. 10 (2010) 1185–1191.
[30] T. Baehr-Jones, M. Hochberg, G. Wang, R. Lawson, Y. Liao, P.A. Sullivan, L. Dalton, A.K.-Y. Jen, A. Scherer, Optical modulation and detection in slotted silicon waveguides, Opt. Express 13 (521) (2005) 6–5226.
[31] G. Wang, T. Baehr-Jones, M. Hochberg, A. Scherer, Design and fabrication of segmented slotted wave-guides for electro-optic modulation, Appl. Phys. Lett. 91 (2007) 143109.
[32] Y. Akahane, T. Asano, B.-S. Song, S. Noda, High-Q photonic nanocavity in a two-dimensional photonic crystal, Nature 425 (2003) 944–947.
[33] T. Tanabe, M. Notomi, E. Kuramochi, A. Shinya, H. Taniyama, Trapping and delaying photons for one nanosecond in an ultrasmall high-Q photonic-crystal nanocavity, Nat. Photonics 1 (2007) 49–52.
[34] K. Nozaki, T. Tanabe, A. Shinya, S. Matsuo, T. Sato, H. Taniyama, M. Notomi, Sub-femtojoule all-optical switching using a photonic-crystal nanocavity, Nat. Photonics 4 (2010) 477–483.
[35] T. Xu, N. Zhu, M.Y.C. Xu, L. Wosinski, J.S. Aitchison, H.E. Ruda, Pillar-array based optical sensor, Opt. Express 18 (2010) 5420–5425.
[36] J. Joannopoulos, R. Meade, J. Winn, Photonic Crystals Molding the Flow of Light, Princeton University Press, Princeton, 1995.
[37] M. Notomi, Manipulating light with strongly modulated photonic crystals, Rep. Prog. Phys. 73 (09650) (2010) 1–096557.
[38] M. Lee, H.E. Katz, C. Erben, D.M. Gill, P. Gopalan, J.D. Heber, D.J. McGee, Broadband modulation of light using an electro-optic polymer, Science 298 (2002) 1401.
[39] T.-D. Kim, J. Lao, Y.-J. Cheng, Z. Shi, S. Hau, S.-H. Jang, X.-H. Zhou, Y. Tian, B. Polishak, S. Huang, H. Ma, L.R. Dalton, A.K.-Y. Jen, Binary chromophore systems in nonlinear optical dendrimers and polymers for large electro-optic activities, J. Phys. Chem. C 112 (2008) 8091–8098.
[40] A. DiFalco, L. O'Faolain, T.F. Krauss, Dispersion control and slow light in slotted photonic crystal waveguides, Appl. Phys. Lett. 92 (2008) 083501–083503.
[41] J.H. Wülbern, S. Prorok, J. Hampe, A. Petrov, M. Eich, J. Luo, A.K.-Y. Jen, M. Jenett, A. Jacob, 40 GHz electro-optic modulation in hybrid silicon–organic slotted photonic crystal waveguides, Opt. Lett. 35 (275) (2010) 3–2755.
[42] C. Kang, C.T. Phare, Y.A. Vlasov, S. Assefa, S.M. Weiss, Photonic crystal slab sensor with enhanced surface area, Opt. Express 18 (2010) 27930–27937.

Biographies

Daquan Yang received the Bachelor's degree of Electronic Information Science and Technology from JiNan University in 2009. He currently is a master candidate in the State Key Laboratory of Information Photonics and Optical Communications, Beijing University of Posts and Telecommunications (BUPT), Beijing, P.R. China. His research now focuses on the area of photonic crystals and optical communication.

Huiping Tian received the B.S. and Ph.D. degrees from Shan xi University, Shanxi, China, in 1998 and 2003, respectively. Now she is an associate professor in the School of Information and Communication Engineering, Beijing University of Posts and Telecommunications (BUPT), Beijing, China. Her research interests are focused on the area of ultra-short and ultra-fast process in the transmission of optics, photonic crystals and broadband information networking.

Yuefeng Ji received the Ph.D. degree from Beijing University of Posts and Telecommunications (BUPT), Beijing, China. Now he is a professor in BUPT. His research interests are primarily in the area of broadband communication networks and optical communications, with emphasis on key theory, realization of technology and applications.